Supplementary Information

# Calcium Pyrenide: A Room-Temperature Reagent for Stoichiometric Calciations and Reductive $Ca^{2+}$ Intercalation Reactions

Anda Wang[†,1], Ryan S. Storteboom[†,1], Shain Sagar Mollick[†], Serhii Vasylevskyi[†], Michael L. Aubrey[†,*]

[†]Department of Chemistry, The University of Texas at Austin, Austin, TX 78712, USA.
[1]Authors contributed equally

## Table of Contents

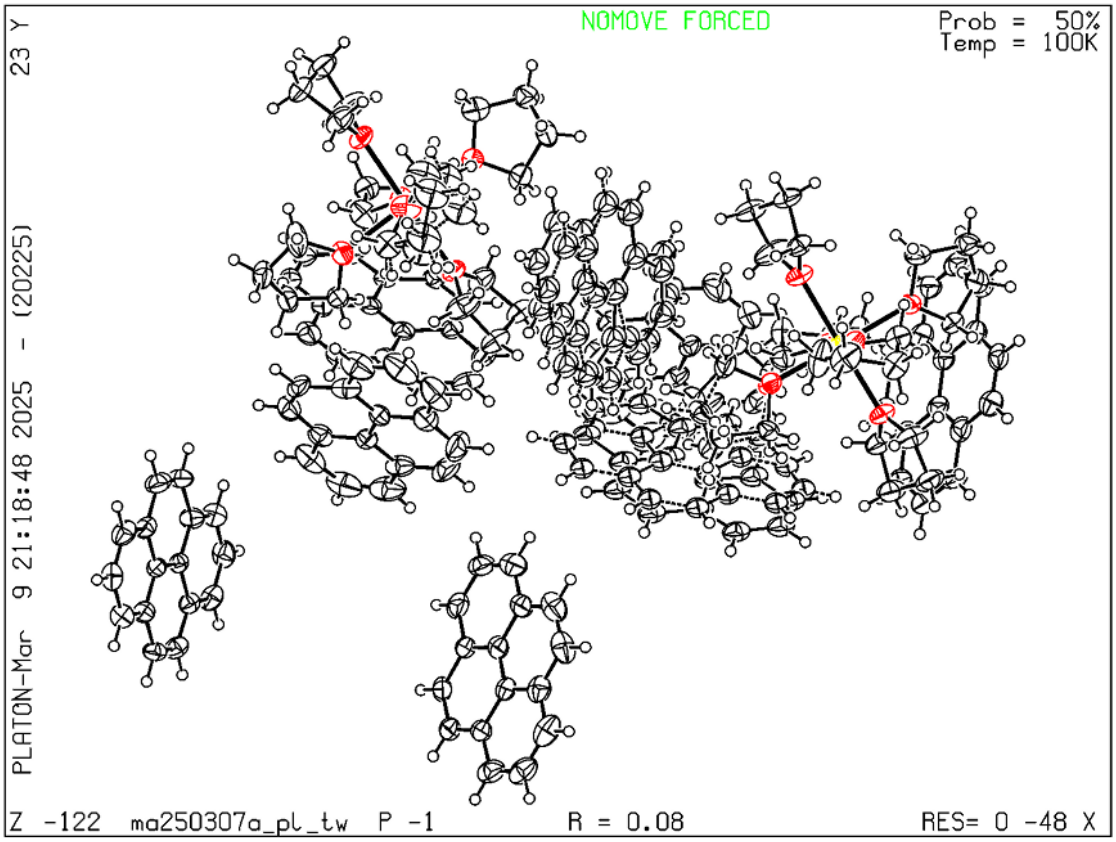


**Figure S1.** Asymmetric unit for $Ca(THF)_6(pyrene)_2(pyrenide^{\bullet-})_2$.

**Table S1.** Crystallographic data for $Ca(THF)_6(pyrene)_2(pyrenide^{\bullet-})_2$

| | |
|---|---|
| Compound | $Ca(THF)_6(pyrene)_2(pyrenide^{\bullet-})_2$ |
| Empirical Formula | C88H88CaO6 |
| Formula weight (g/mol) | 1281.66 |
| Temperature (K) | 100 |
| Crystal system | Triclinic |
| Space group | P-1 |
| *a* (Å) | 14.6514(2) |
| *b* (Å) | 21.4427(4) |
| *c* (Å) | 21.4763(5) |
| Volume (Å$^3$) | 6728.1(2) |
| Z | 4 |
| Density, calc. (g/cm$^3$) | 1.265 |
| Absorption coefficient (mm$^{-1}$) | 1.254 |
| *F*(000) | 2736 |
| Radiation | Cu Kα (λ=1.54184 Å) |
| Completeness to $\theta_{max}$ | 67.684 |
| Data/restraints/parameters | 24815/1056/2022 |
| Goodness-of-fit on $F^2$ | 1.062 |
| Final R indices [$I>2\sigma(I)$][a] | $R_1 = 0.0752$, w$R_2 = 0.1956$ |
| Largest diff. peak/hole (e/Å$^3$) | 0.612 |

[a] $R_1 = \Sigma||F_o| - |F_c||/\Sigma|F_o|$, $wR_2 = [\Sigma w(F_o^2 - F_c^2)^2/\Sigma(F_o^2)^2]^{1/2}$

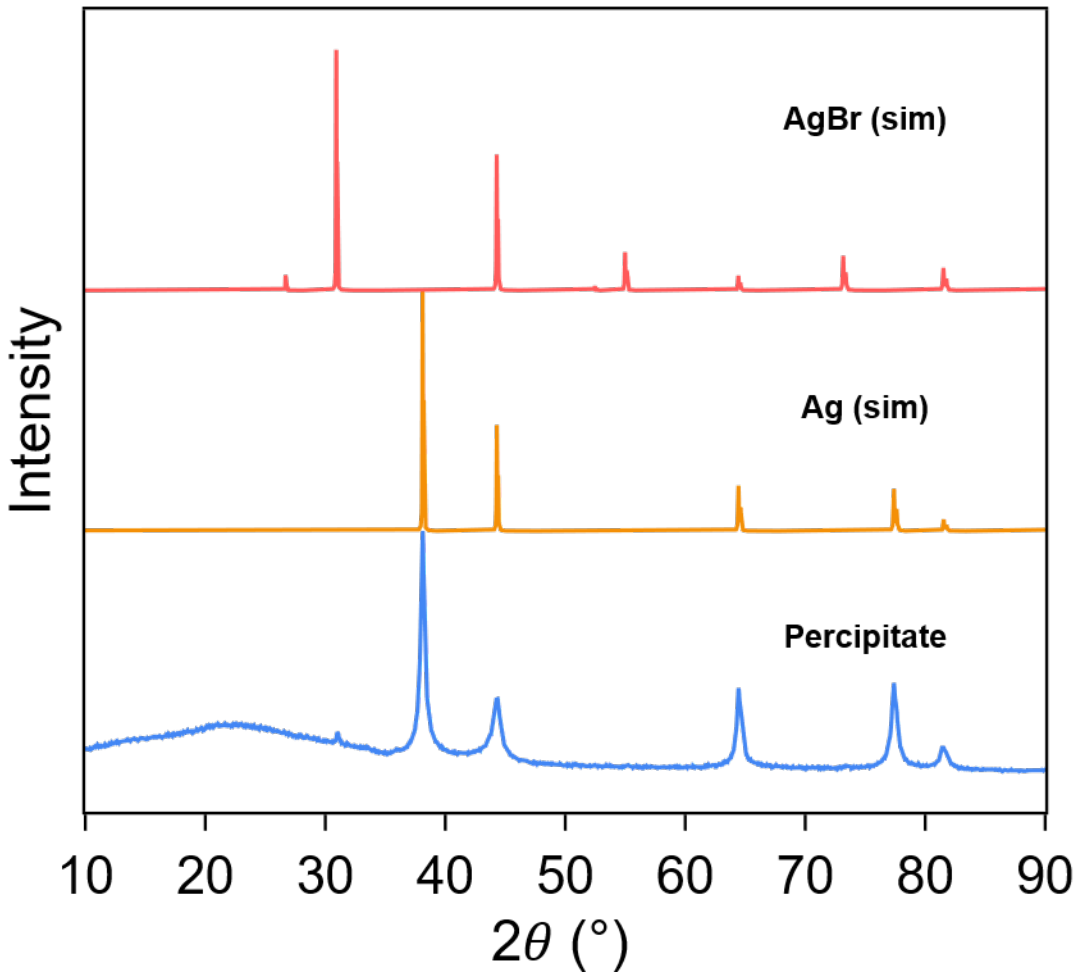


**Figure S2.** PXRD pattern for Ag deposition product (blue) and simulated PXRD patterns from Ag (yellow) and AgBr (red) references.[41,42]

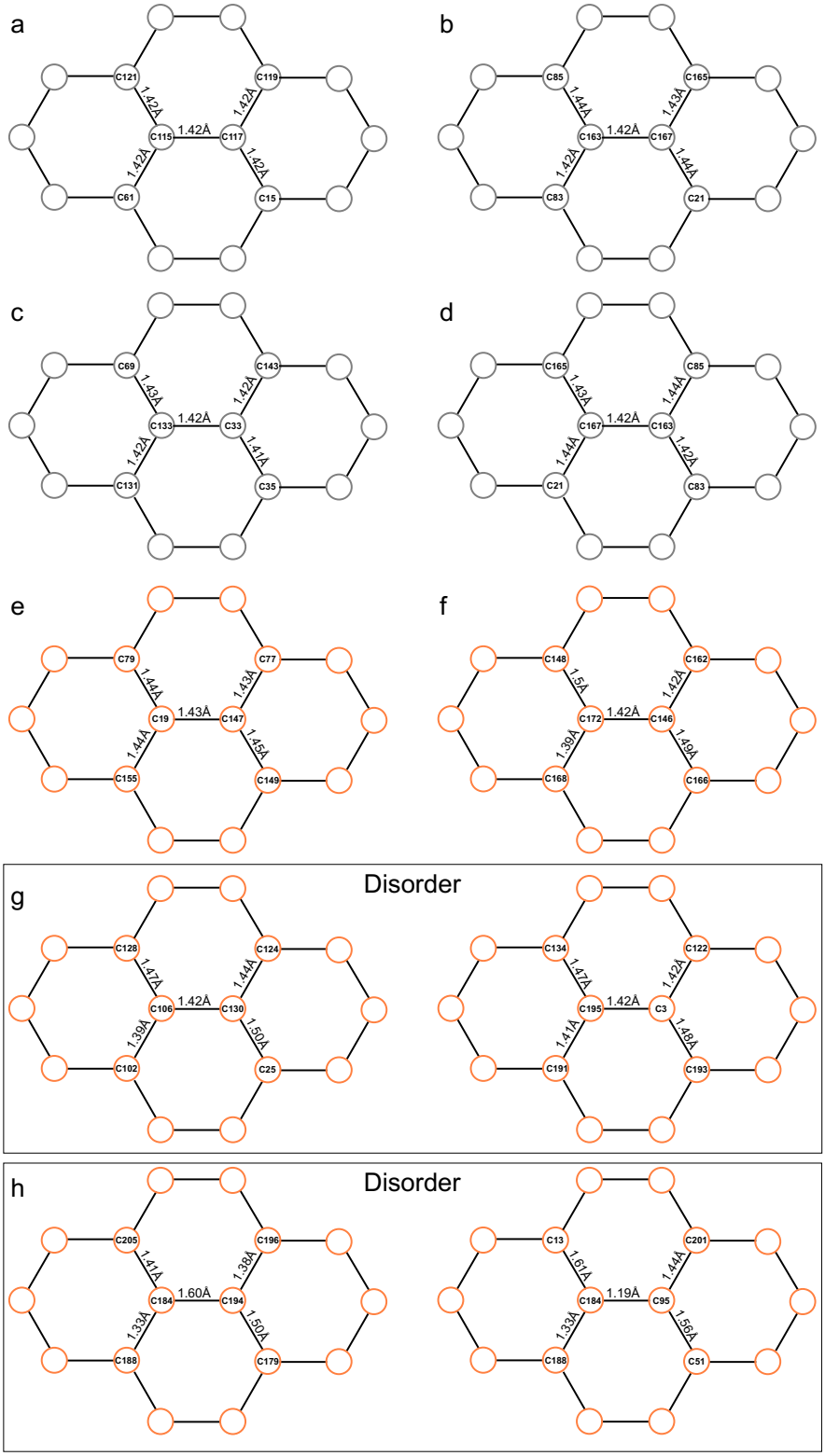


**Figure S3.** Illustration of pyrene (a–d) and pyrenide (e–h) molecules present in the asymmetric unit of the $Ca(THF)_6(pyrene)_2(pyrenide^{\bullet-})_2$ crystal structure. Bond lengths of each corresponding inner ring tertiary carbons are labeled. Bond length estimates from the disordered pyrenide rings were not included in the statistical analysis presented in the main text.

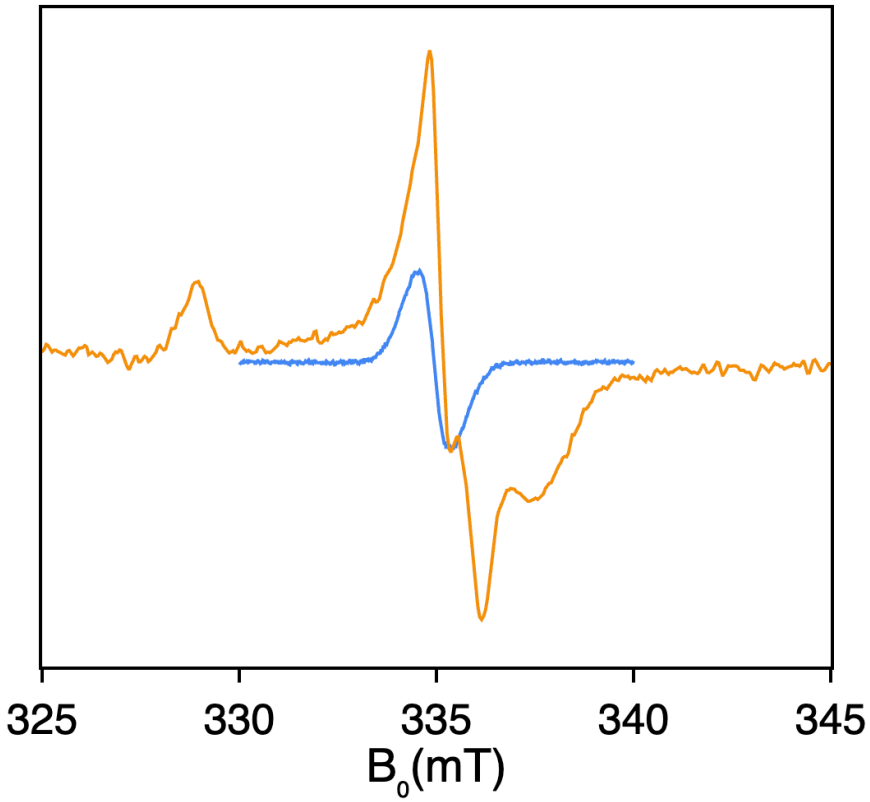


**Figure S4**. EPR of the product solution following reaction of excess pyrene with calcium and 8.5 mol% 1,2-dibromoethane in THF. Spectra were collected at room temperature (blue) and 106 K (orange).

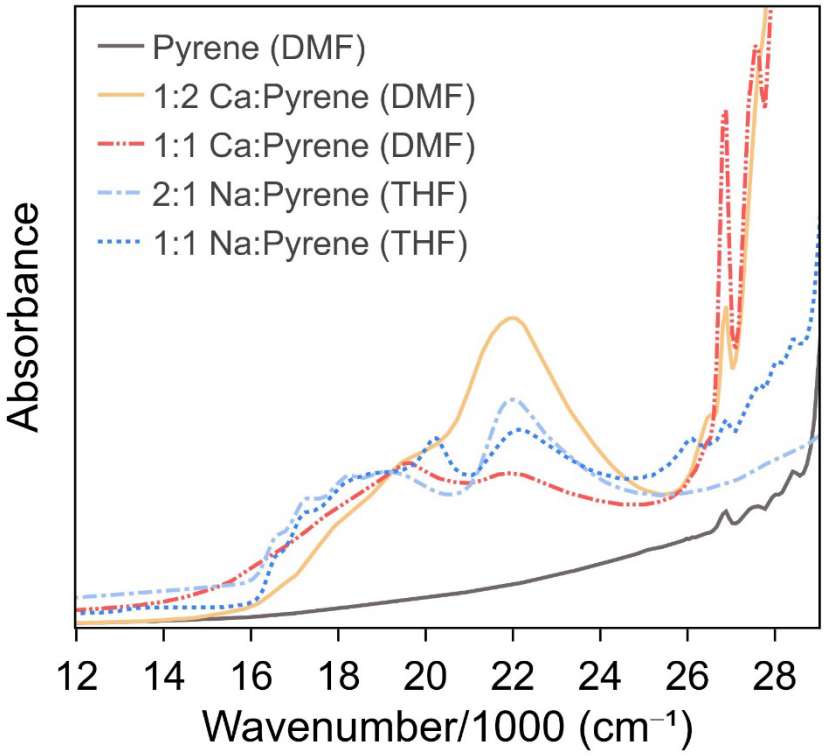


**Figure S5.** UV-*vis* absorption spectra of pyrene (grey, solid), pyrene solution reacted with ½ equivalent (light orange, solid) and 1 equivalent (red, dash-dot-dot) of calcium in DMF, and with 2 equivalents (light blue, dash-dot) and 1 equivalent (blue, dot) of sodium in THF.

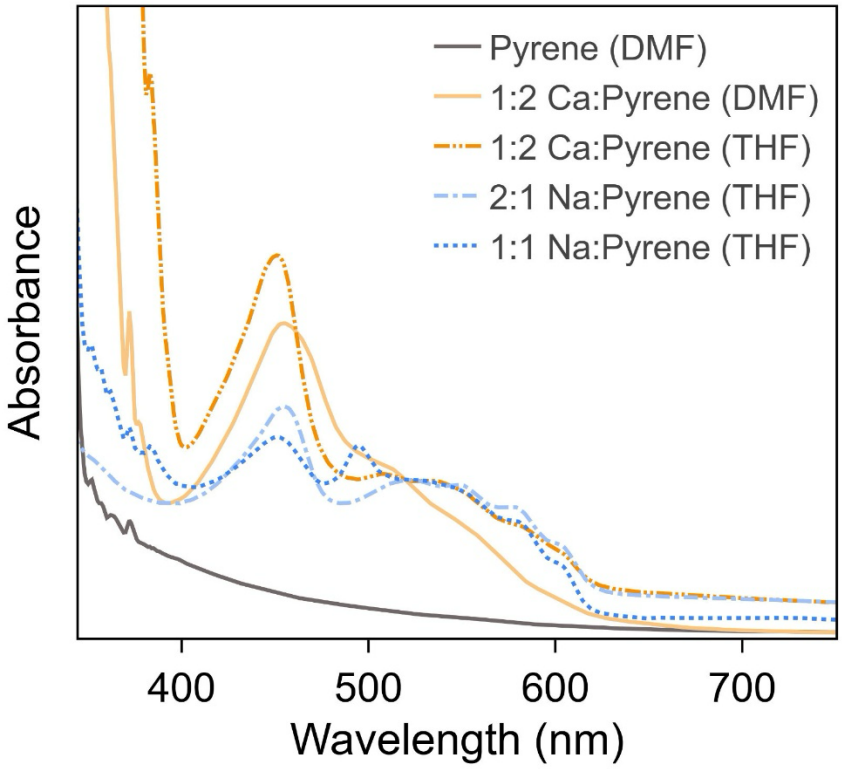


**Figure S6.** UV-*vis* absorption spectra of pyrene in DMF (grey, solid), a pyrene solution reacted with ½ equivalent of calcium in DMF (light orange, solid) and THF (orange, dash-dot-dot), and pyrene reacted with 2 equivalents (light blue, dash-dot) and 1 equivalent (blue, dot) of sodium in THF.

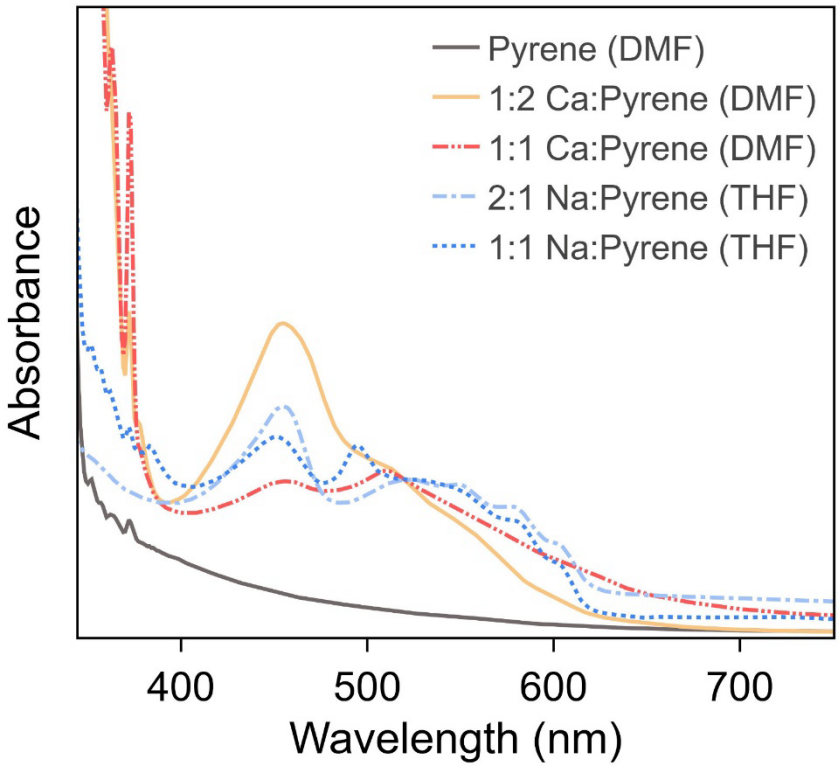


**Figure S7.** UV-*vis* absorption spectra of pyrene (grey, solid), pyrene solution reacted with ½ equivalent (light orange, solid) and 1 equivalent (red, dash-dot-dot) of calcium in DMF, and with 2 equivalents (light blue, dash-dot) and 1 equivalent (blue, dot) of sodium in THF.

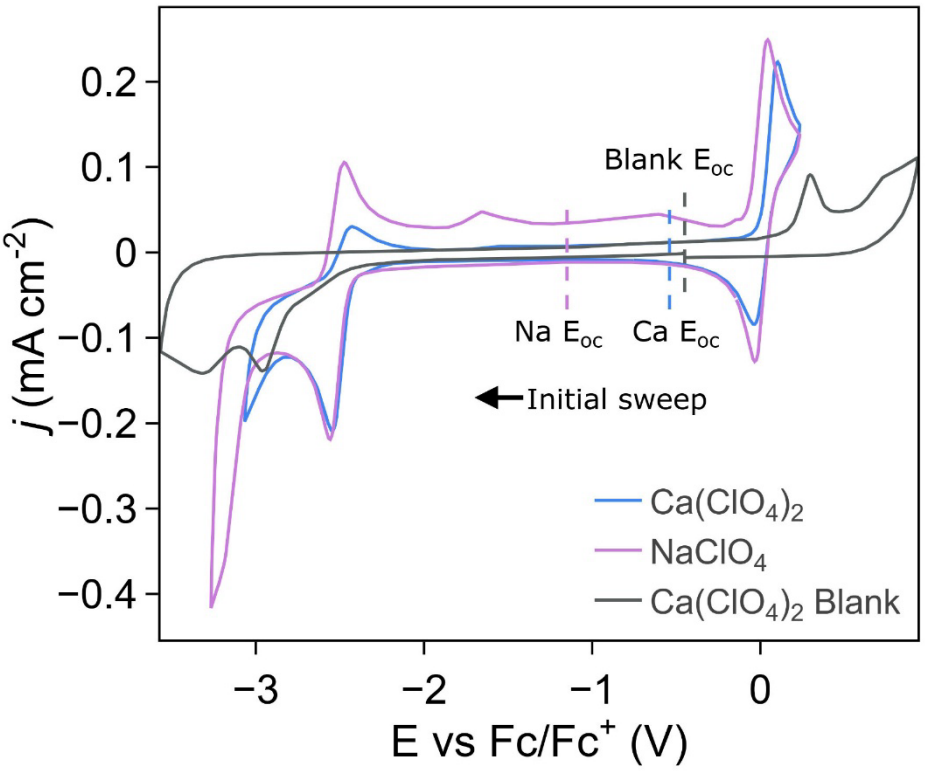


**Figure S8**. CV with electrochemical stability window, showing an expanded negative window for 1 mM pyrene, 1 mM ferrocene, and 0.1 M $Ca(ClO_4)_2$ (blue) or 0.1 M $NaClO_4$ (purple). The pure electrolyte solution, 0.1 M $Ca(ClO_4)_2$, is shown in grey.

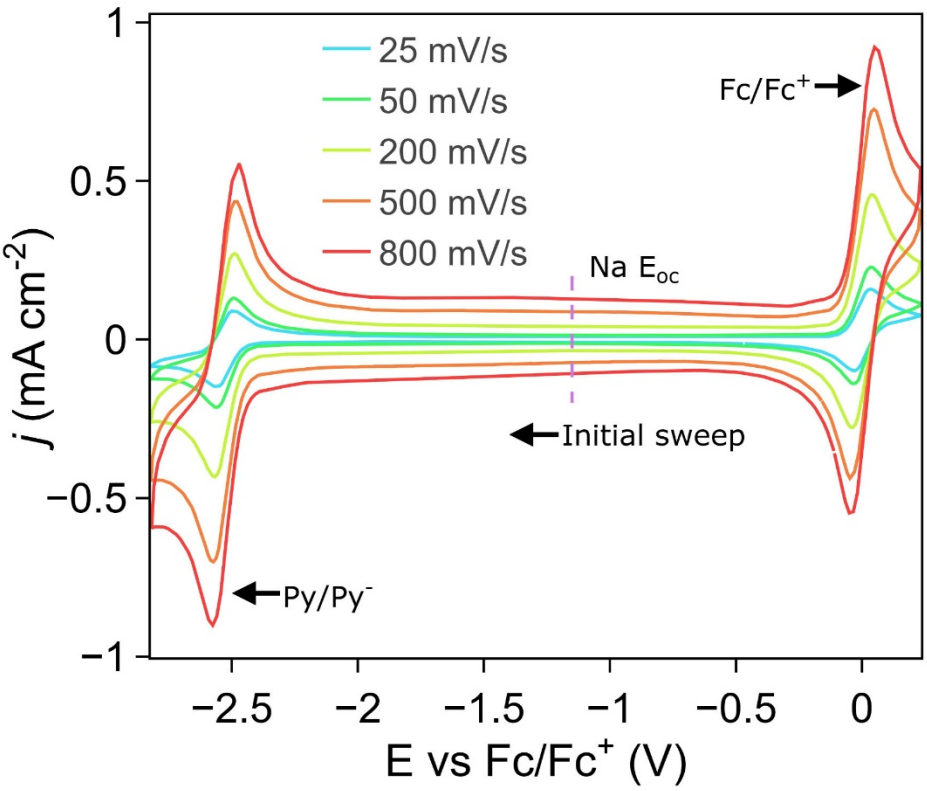


**Figure S9.** Cyclic voltammogram of 1 mM pyrene, 1 mM ferrocene, and 0.1 M $NaClO_4$ in DMF collected using a glassy carbon working electrode, platinum wire counter electrode, and silver / silver nitrate reference electrode at various scan rates.

**Table S2.** Peak potentials (*E)* and peak separations (*ΔE*) for 1 mM pyrene and 1 mM ferrocene within a 0.1 M $NaClO_4$ DMF electrolyte solution at various scan rates.

| | $Py/Py^-$ | | | $Fc/Fc^+$ | | |
|---|---|---|---|---|---|---|
| $\nu$ (mV/s) | $E_{red}$ (V) | $E_{ox}$ (V) | $\Delta E$ (mV) | $E_{red}$ (V) | $E_{ox}$ (V) | $\Delta E$ (mV) |
| 25 | –2.5579 | –2.4911 | 67 | –0.0344 | 0.0344 | 69 |
| 50 | –2.5566 | –2.4868 | 70 | –0.0341 | 0.0341 | 68 |
| 200 | –2.5666 | –2.4885 | 78 | –0.0355 | 0.0355 | 71 |
| 500 | –2.5726 | –2.4784 | 94 | –0.0475 | 0.0475 | 95 |
| 800 | –2.5756 | –2.4706 | 105 | –0.0501 | 0.0501 | 100 |

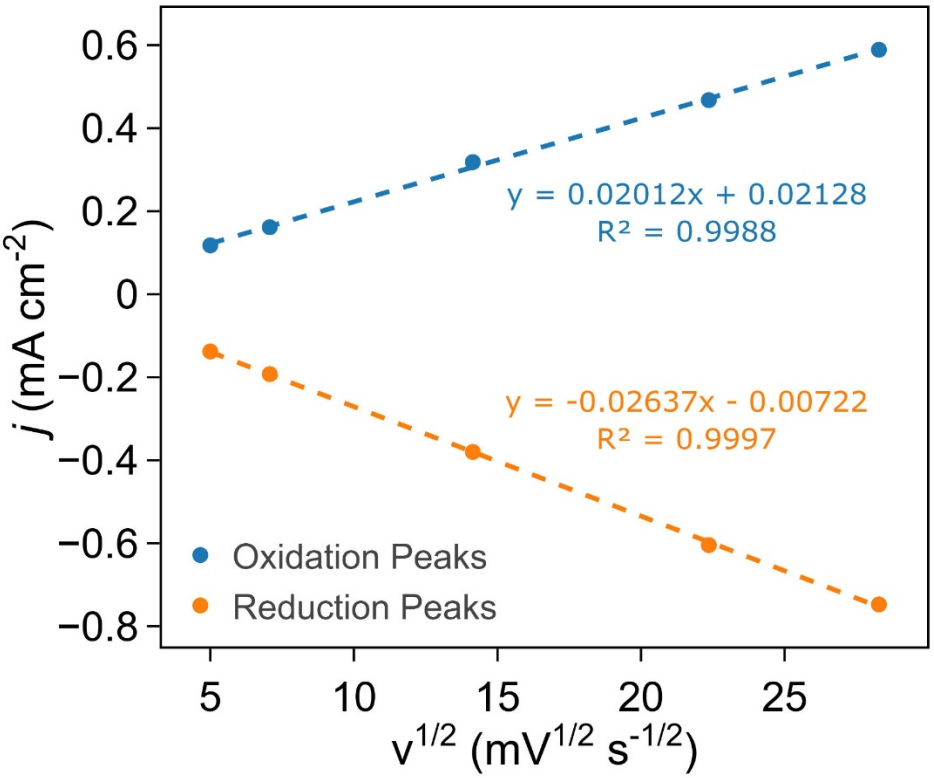


**Figure S10.** Oxidation and reduction peak currents for the pyrene/pyrene$^{-}$ redox couple.

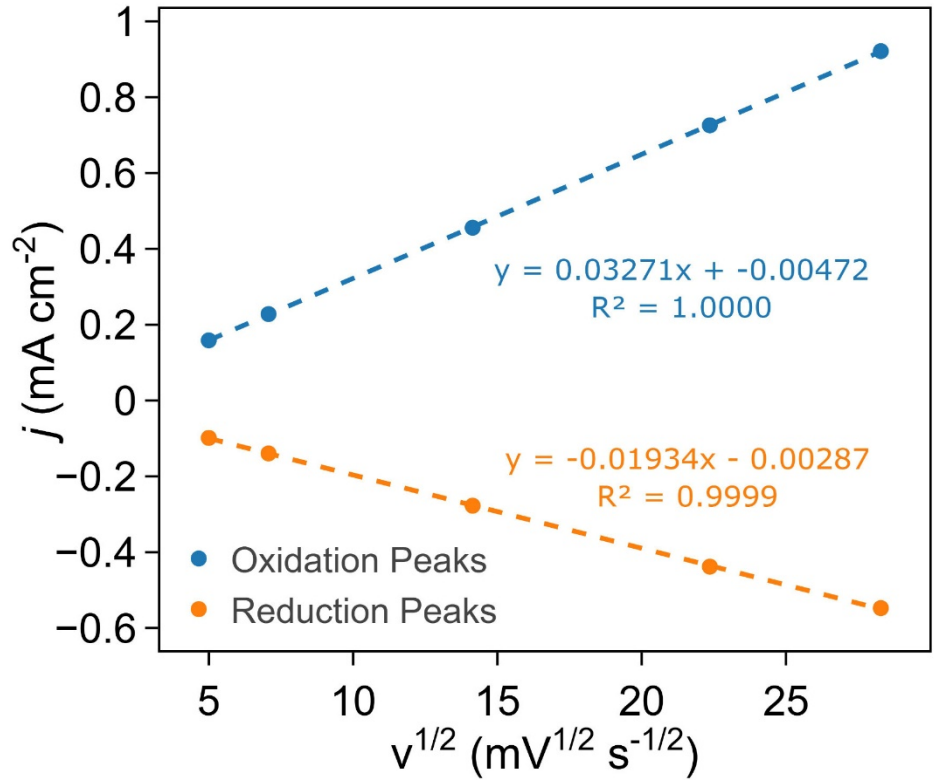


**Figure S11.** Oxidation and reduction peak currents for the Fc/Fc$^{+}$ redox couple.

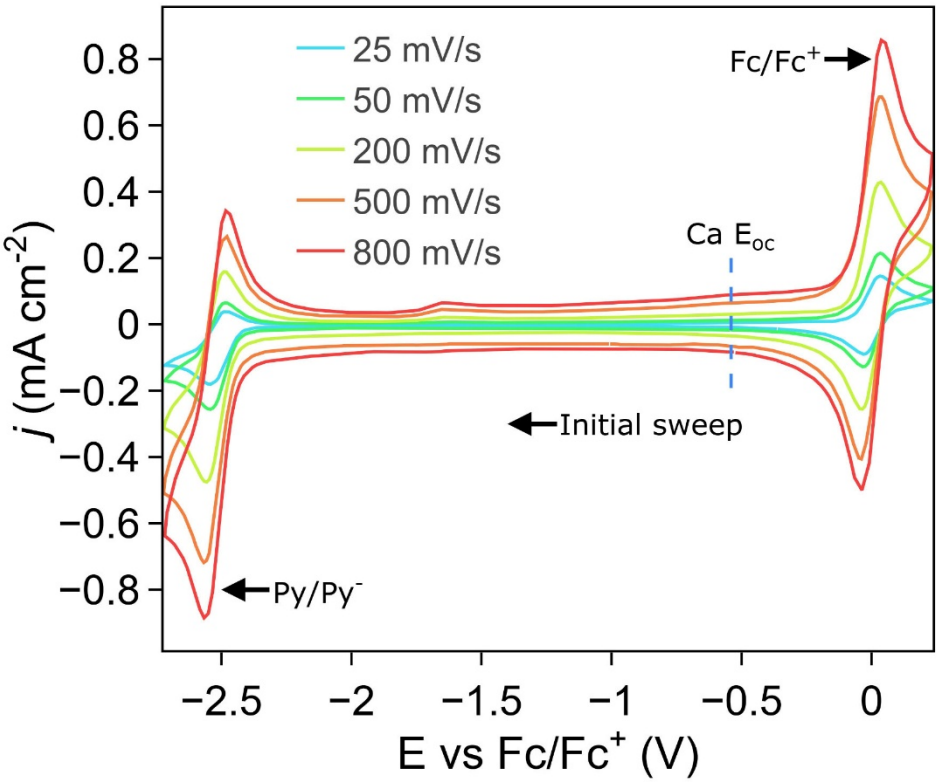


**Figure S12.** Cyclic voltammogram of 1 mM pyrene, 1 mM ferrocene, 0.1 M $Ca(ClO_4)_2$ in DMF collected using a glassy carbon working electrode, Pt wire counter electrode, and $Ag/AgNO_3$ reference electrode at various scan rates.

**Table S3.** Peak potentials (*E)* and peak separations (*ΔE*), for 1 mM pyrene and 1 mM ferrocene in a 0.1 M $Ca(ClO_4)_2$ DMF electrolyte solution at various scan rates.

| | Py/Py⁻ | | | Fc/Fc⁺ | | |
|---|---|---|---|---|---|---|
| *ν* (mV/s) | $E_{red}$ (V) | $E_{ox}$ (V) | *ΔE* (mV) | $E_{red}$ (V) | $E_{ox}$ (V) | *ΔE* (mV) |
| 25 | –2.5412 | –2.4795 | 62 | –0.0321 | 0.0321 | 64 |
| 50 | –2.5422 | –2.4872 | 55 | –0.0340 | 0.0340 | 68 |
| 200 | –2.5565 | –2.4908 | 66 | –0.0358 | 0.0358 | 72 |
| 500 | –2.5674 | –2.4784 | 89 | –0.0391 | 0.0391 | 78 |
| 800 | –2.5663 | –2.4828 | 84 | –0.0372 | 0.0372 | 74 |

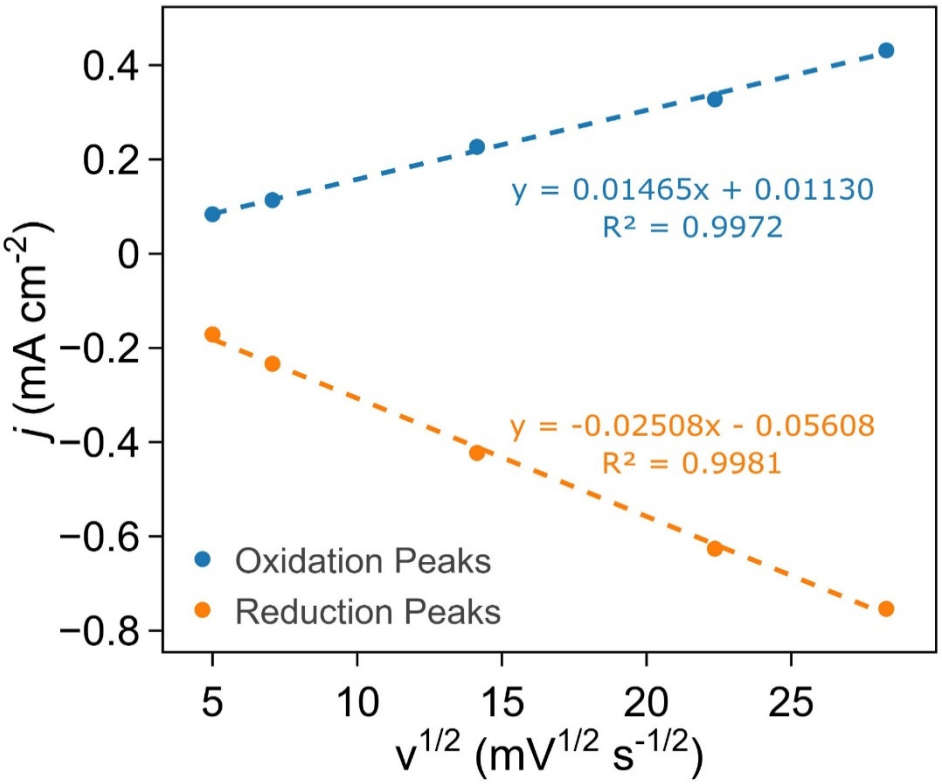


**Figure S13.** Oxidation and reduction peak current densities for the Pyrene/Pyrene$^{-}$ redox couple.

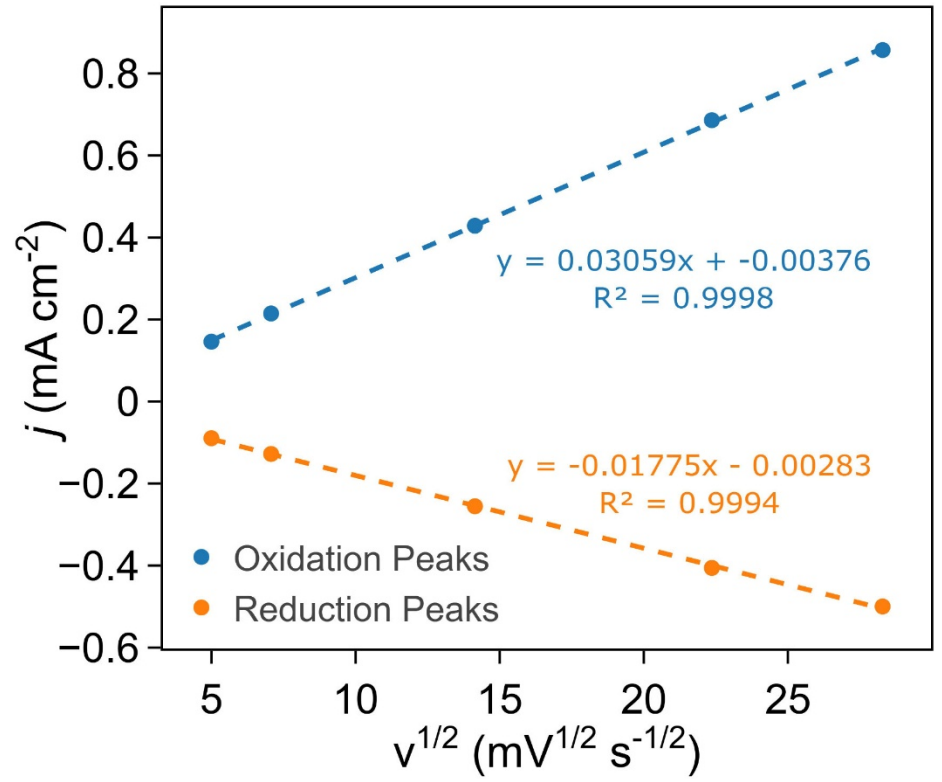


**Figure S14.** Oxidation and reduction peak currents for the Fc/Fc$^{+}$ redox couple.

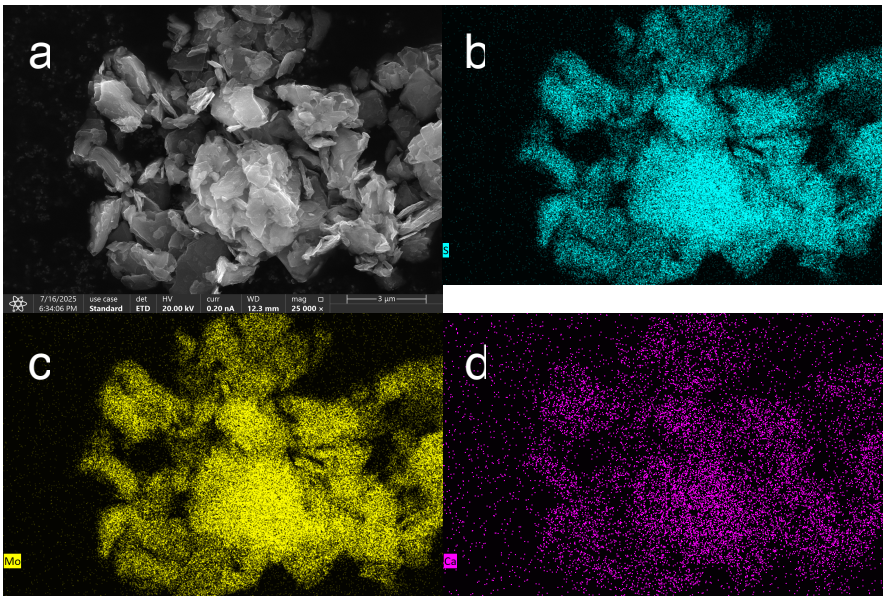


**Figure S15.** (a) SEM image of $MoS_2$ after reaction with 0.3 equivalents of calcium pyrenide in DMF and elemental mapping of (b) S, (c) Mo, and (d) Ca.

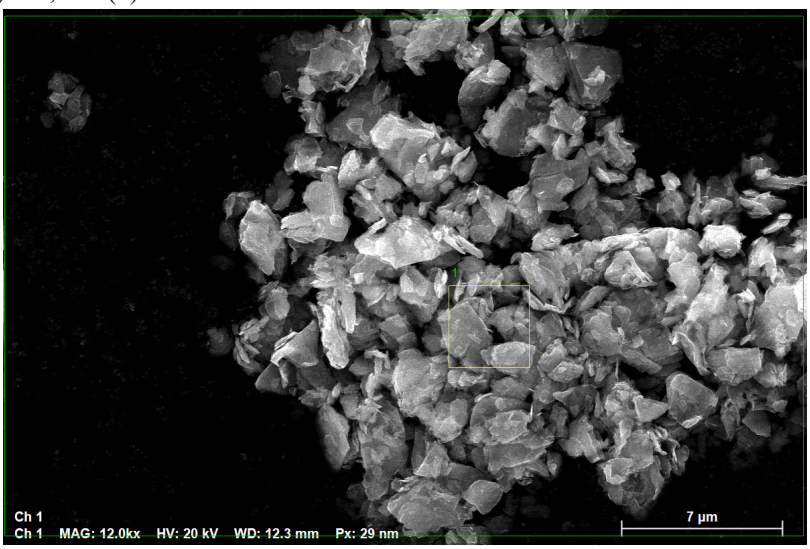


**Figure S16.** EDX spot of $MoS_2$ after reaction with 0.3 equivalents of calcium pyrenide in DMF.

**Table S4.** Elemental analysis from the EDX spot in Figure S15 for $MoS_2$ after reaction with 0.3 equivalents of calcium pyrenide in DMF.

| Element | Counts | Atom percent (%) | 1σ Uncertainty (%) |
|---|---|---|---|
| Carbon | 301 | 70.24 | 2.41 |
| Oxygen | 85 | 9.36 | 0.91 |
| Sulfur | 4859 | 12.85 | 2.05 |
| Calcium | 420 | 2.24 | 0.48 |
| Molybdenum | 3674 | 5.31 | 4.59 |

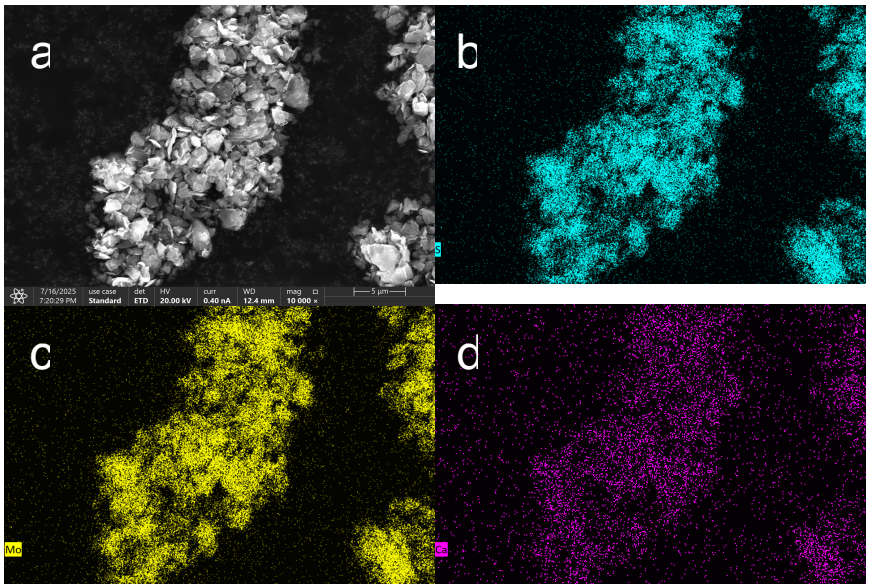


**Figure S17.** (a) SEM image of $MoS_2$ after reaction with 0.5 equivalents of calcium pyrenide in DMF and elemental mapping of (b) S, (c) Mo, and (d) Ca.

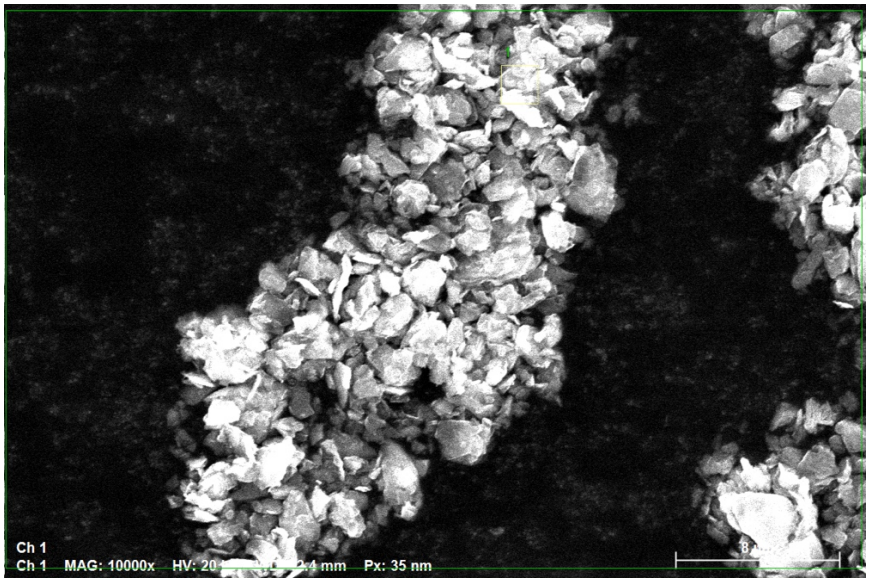


**Figure S18.** EDX spot of $MoS_2$ after reaction with 0.5 equivalents of calcium pyrenide in DMF.

**Table S5.** Elemental analysis from the EDX spot in Figure S17 for $MoS_2$ after reaction with 0.5 equivalents of calcium pyrenide in DMF.

| Element | Counts | Atom percent (%) | 1σ Uncertainty (%) |
|---|---|---|---|
| Carbon | 235 | 86.83 | 4.57 |
| Oxygen | 15 | 4.73 | 1.63 |
| Sulfur | 693 | 4.99 | 2.57 |
| Calcium | 86 | 1.21 | 0.76 |
| Molybdenum | 600 | 2.24 | 5.87 |

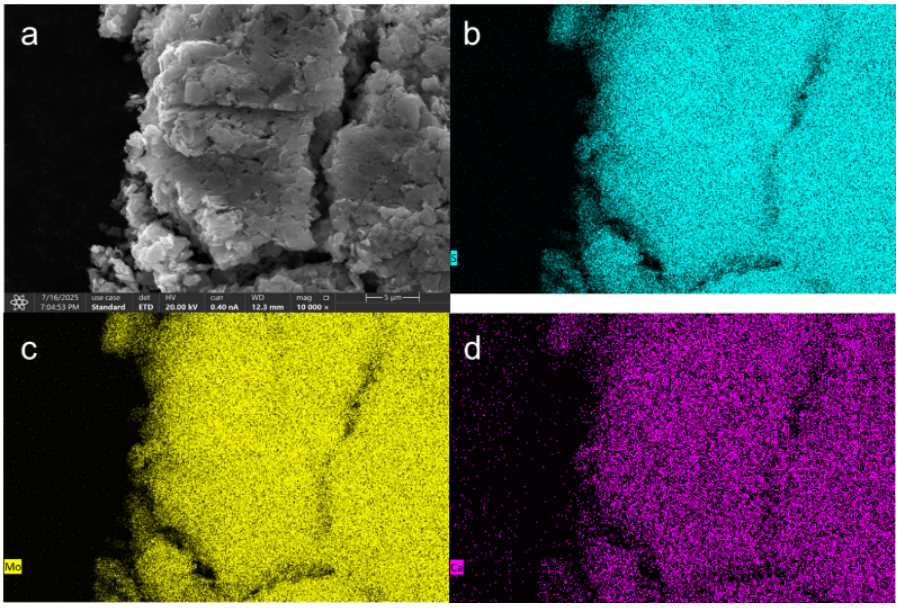


**Figure S19.** (a) SEM image of $MoS_2$ after reaction with 0.7 equivalents of calcium pyrenide in DMF and elemental mapping of (b) S, (c) Mo, and (d) Ca.

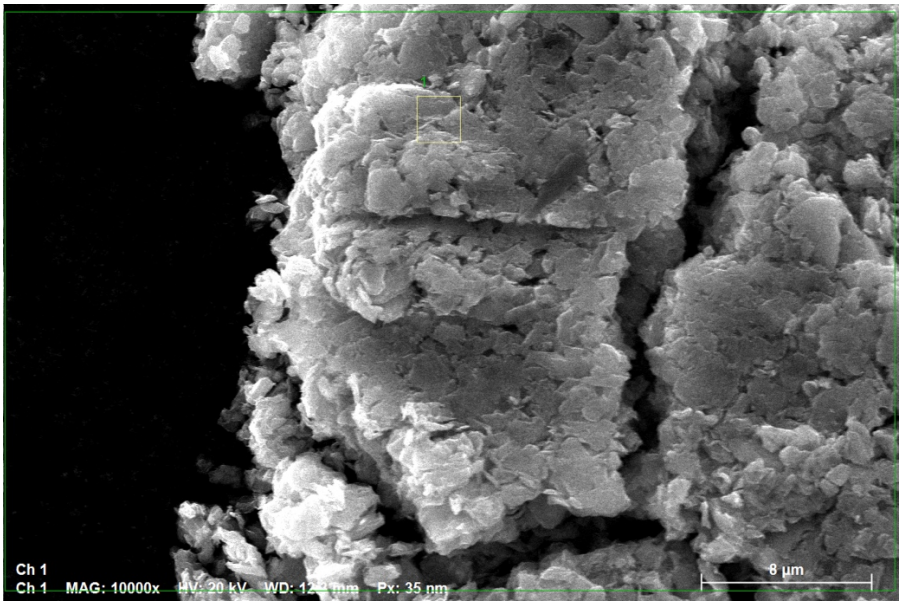


**Figure S20.** EDX spot of $MoS_2$ after reaction with 0.7 equivalents of calcium pyrenide in DMF.

**Table S6.** Elemental analysis from the EDX spot in Figure S19 for $MoS_2$ after reaction with 0.7 equivalents of calcium pyrenide in DMF.

| Element | Counts | Atom percent (%) | 1σ Uncertainty (%) |
|---|---|---|---|
| Carbon | 117 | 59.24 | 2.40 |
| Oxygen | 81 | 17.25 | 1.18 |
| Sulfur | 2715 | 14.44 | 2.10 |
| Calcium | 335 | 4.20 | 0.85 |
| Molybdenum | 1696 | 4.87 | 5.01 |

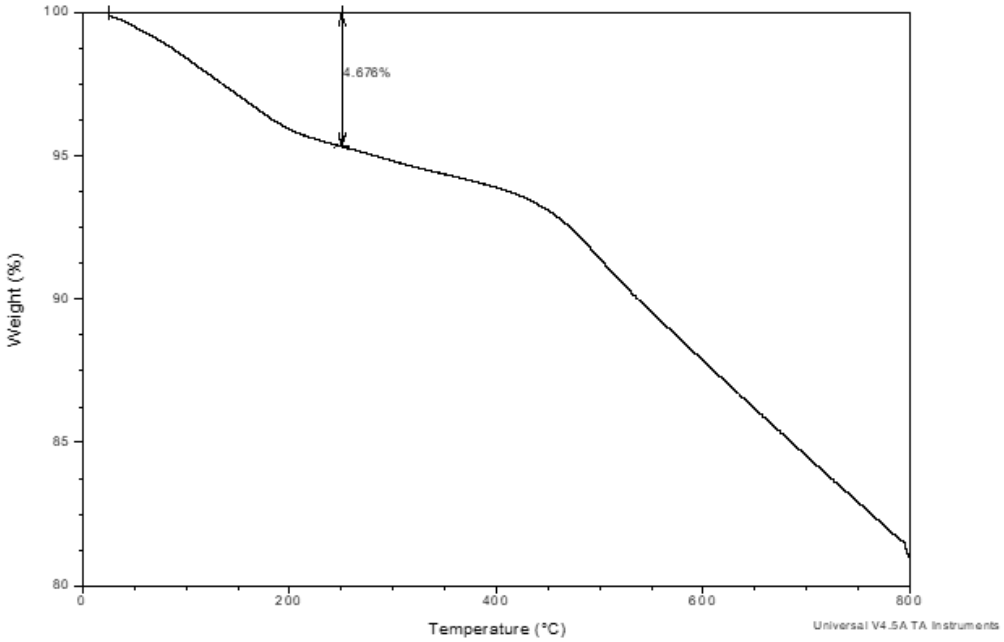


**Figure S21.** TGA of $MoS_2$ after reaction with 0.3 equivalents of calcium pyrenide in DMF.

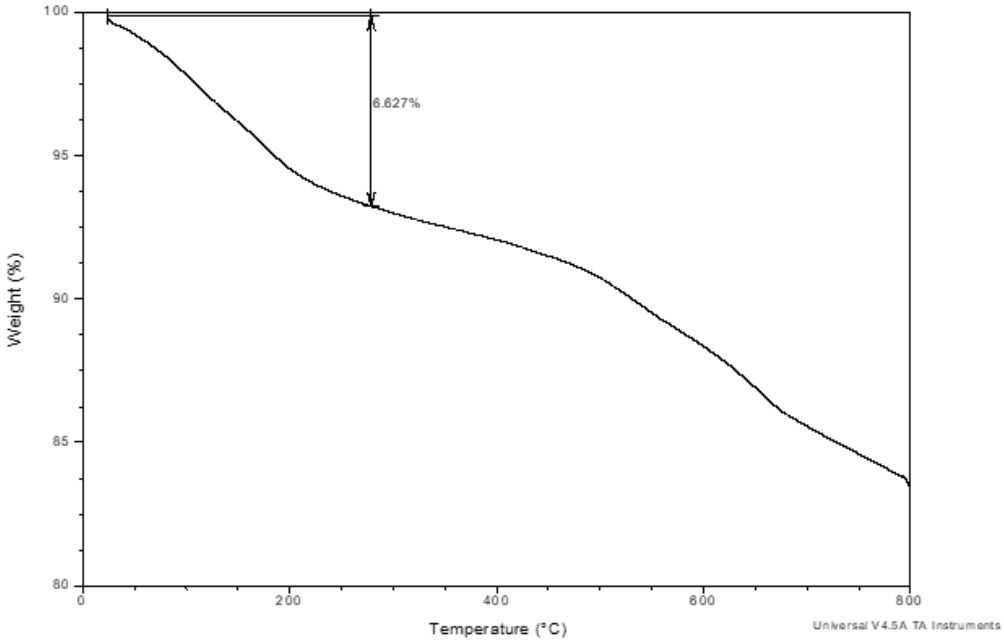


**Figure S22.** TGA of $MoS_2$ after reaction with 0.5 equivalents of calcium pyrenide in DMF.

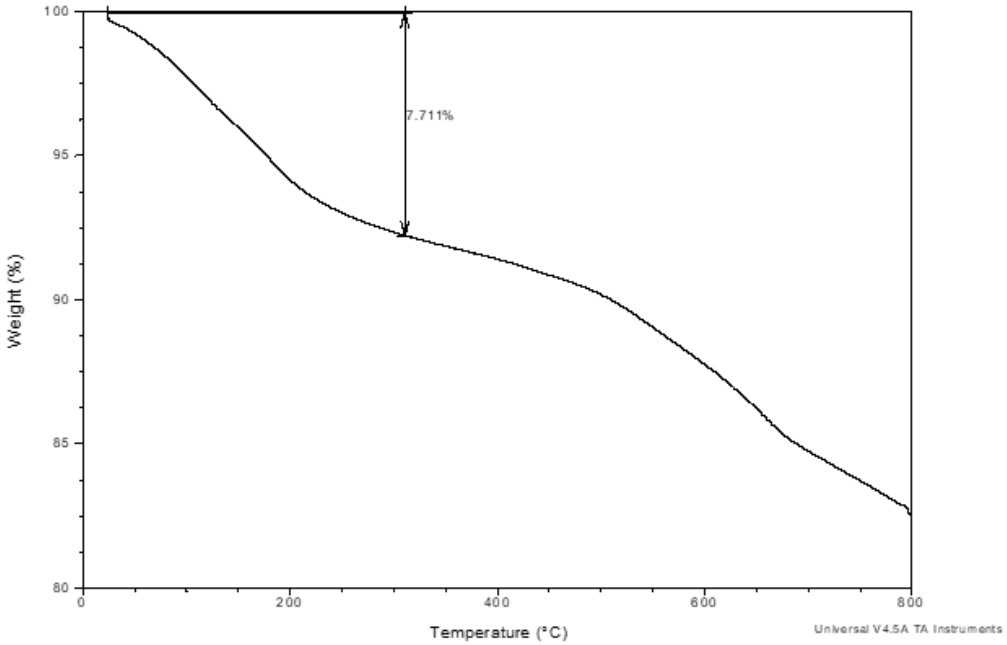


**Figure S23.** TGA of $MoS_2$ after reaction with 0.7 equivalents of calcium pyrenide in DMF.

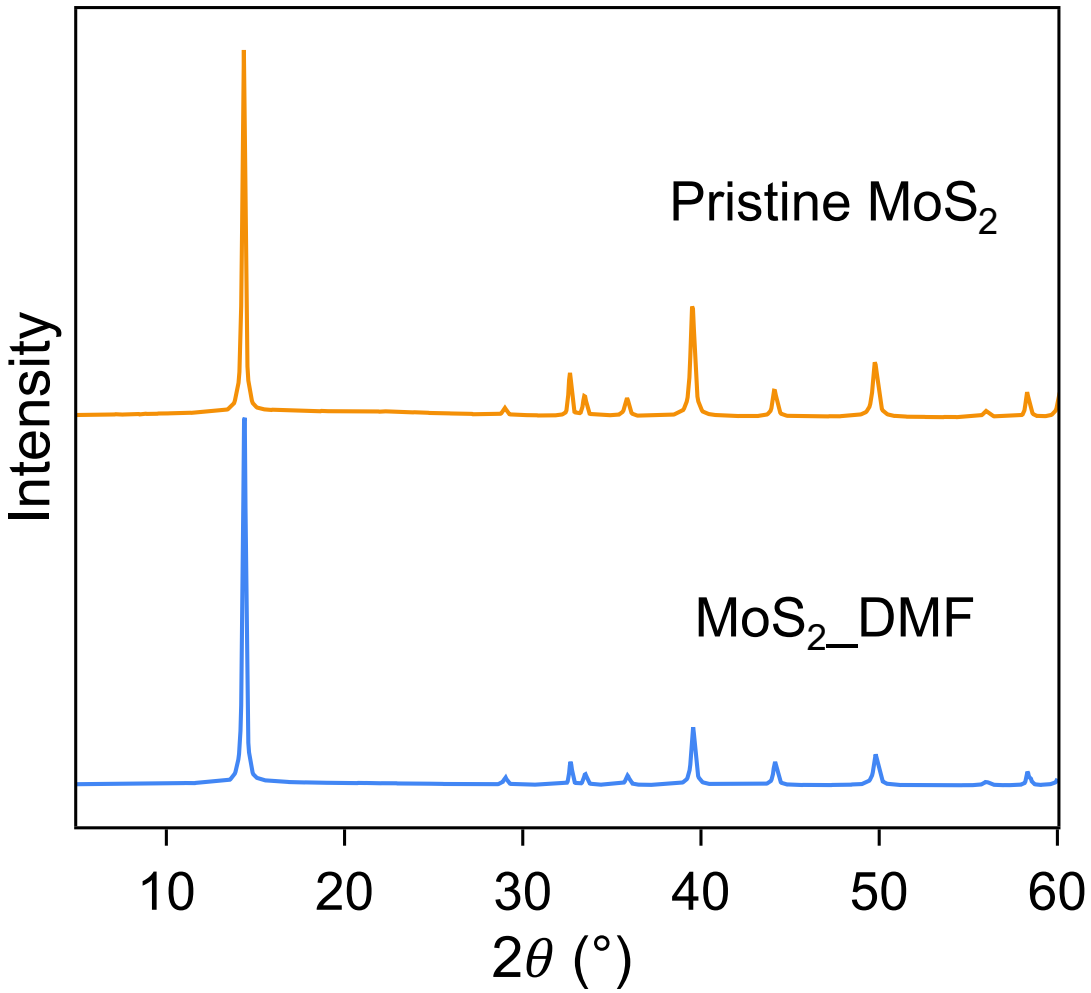


**Figure S24.** PXRD pattern of pristine $MoS_2$ (orange) and $MoS_2$ after stirring in DMF for 24 h (blue).

## References

(41) Wilsey, R. B. LIII. The Crystalline Structures of Silver Iodide. *Lond. Edinb. Dublin Philos. Mag. J. Sci.* **1923**, *46* (273), 487–496. https://doi.org/10.1080/14786442308634272.

(42) Vegard, L. IX. The Structure of Silver Crystals. *Lond. Edinb. Dublin Philos. Mag. J. Sci.* **1916**, *31* (181), 83–87. https://doi.org/10.1080/14786440108635473.